

Water Distribution in Multilayers of Weak Polyelectrolytes

Oleh M. Tanchak,[†] Kevin G. Yager,[†] Helmut Fritzsche,[‡] Thad Harroun,^{‡,§}
John Katsaras,^{‡,⊥} and Christopher J. Barrett^{*,†}

Department of Chemistry, McGill University, Montreal, Canada, Canadian Neutron Beam Centre,
National Research Council, Chalk River, Canada, Department of Physics, University of Guelph,
Guelph, Canada, and ⁴Guelph-Waterloo Physics Institute and the Biophysics Interdepartmental Group,
University of Guelph, Guelph, Ontario, Canada

Received November 3, 2005. In Final Form: April 2, 2006

The water localization in thin polyelectrolyte multilayers assembled from poly(acrylic acid) and poly(allylamine hydrochloride) was investigated with neutron reflectivity in an atmosphere of controlled humidity and with bulk water. Water was found to be distributed asymmetrically within the multilayer and to localize preferentially at the polymer surface. The diffusion of water into the multilayer did not completely penetrate to the substrate, but instead there appeared to be an exclusion zone near the Si substrate. These results help to explain previous observations of anomalous water transport kinetics in weak polyelectrolyte systems.

Introduction

Polyelectrolyte multilayers (PEMs) prepared by sequentially dipping a charged substrate into solutions of oppositely charged polyelectrolytes are of interest in many material applications because of their novel properties. Film thickness and surface properties can be controlled in weak polyelectrolyte systems through the regulation of the pH and the ionic strength of the solution through the control of the solution's screening length and the average charge, which modifies the polymer conformation during adsorption.¹ The ease of thin film assembly and the ability to introduce functional groups into the multilayers makes PEMs suitable for applications such as sensors,^{2–4} separation membranes,^{5–7} and drug delivery vehicles.^{4,8–11} However, the ionic character of the internal cross-link points and free acid/base groups makes their interaction with water complex. Recently it was found that PEM preexposure to various humidity environments can greatly influence bulk water uptake, where the rate of swelling could be varied by 3 orders of magnitude on the basis of the relative humidity (RH) prior to exposure to bulk water.¹² Films preexposed to high humidity required a longer time to reach saturation when swollen with bulk water. This observation is counter-intuitive since one might expect that preexposure to high

levels of water vapor could plasticize the multilayer and accelerate the rate of swelling. The sensitivity of PEMs to water vapor content may be attributed to structural changes in the film and/or water organization within the film, and knowledge of the hydration properties and the water distribution within the PEM is of great importance to many applications.

Studies on the build-up of PEMs have shown that fully charged PEM systems composed of polystyrene sulfonate/polyallylamine can be subdivided into three regions of gradual transitions.¹³ The first region is typically composed of a few dense layers that are influenced by the underlying substrate. The second bulk zone consists of polyanion/polycation layers of 1:1 stoichiometry, and the third outer region contains a few layers that are charge overcompensated, which enables the adsorption of additional layers. Neutron reflectivity studies have proven to be a powerful method to characterize the internal structure of PEM in terms of their polymer density and water content,^{14,15} and it has been shown that the internal structure of the PEM layers are highly interpenetrated and that initially deposited layers are thinner than the bulk.^{14,15} Other studies have shown that a density gradient of the polyelectrolyte chains occurs within PEMs when exposed to D₂O.¹⁶ Neutron reflectivity studies have also been used to determine Flory–Huggins interaction parameters.¹⁷ However, these previous studies did not elucidate the water distribution within the multilayer. In this paper, we provide a direct measurement of water association inside weak poly(acrylic acid) and poly(allylamine hydrochloride) (PAA/PAH) PEMs. The water distribution in PAA/PAH assembled films was measured when exposed to water both as vapor and in the bulk, using neutron reflectivity. These experiments provide insight into the sensitivity of the swelling dynamics of the multilayers to water vapor and understanding of the water distribution within the film, which could aid in further technological applications of these films. The determination of the water distribution within the films was

* To whom correspondence should be addressed. E-mail: christopher.barrett@mcgill.ca.

[†] McGill University.

[‡] National Research Council.

[§] Department of Physics, University of Guelph.

[⊥] Guelph-Waterloo Physics Institute and the Biophysics Interdepartmental Group, University of Guelph.

(1) Decher, G. *Science* **1997**, *277*, 1232.

(2) Lee, S.-H.; Kumar, J.; Tripathy, S. K. *Langmuir* **2000**, *16*, 10482.

(3) Dai, J.; Jensen, A. W.; Mohanty, D. K.; Erndt, J.; Bruening, M. L. *Langmuir* **2001**, *17*, 931.

(4) Zhai, L.; Nolte, A. J.; Cohen, R. E.; Rubner, M. F. *Macromolecules* **2004**, *37*, 6113.

(5) Dai, J.; Balachandra, A. M.; Lee, J. I.; Bruening, M. L. *Macromolecules* **2002**, *35*, 3164.

(6) Jin, W.; Toutianoush, A.; Tieke, B. *Langmuir* **2003**, *19*, 2550.

(7) Miller, M. D.; Bruening, M. L. *Langmuir* **2004**, *20*, 11545.

(8) Shi, X.; Caruso, F. *Langmuir* **2001**, *17*, 2036.

(9) Sukhorukov, G. B.; Antipov, A. A.; Voigt, A.; Donath, E.; Mohwald, H. *Macromol. Rapid Commun.* **2001**, *22*, 44.

(10) Chung, A. J.; Rubner, M. F. *Langmuir* **2002**, *18*, 1176.

(11) Nolan, C. M.; Serpe, M. J.; Lyon, L. A. *Biomacromolecules* **2004**, *5*, 1940.

(12) Tanchak, O. M.; Barrett, C. J. *Chem. Mater.* **2004**, *16*, 2734.

(13) Ladam, G.; Schaad, P.; Voegel, J. C.; Schaaf, P.; Decher, G.; Cuisinier, F. *Langmuir* **2000**, *16*, 1249.

(14) Schmitt, J.; Gruenewald, T.; Decher, G.; Pershan, P. S.; Kjaer, K.; Loesche, M. *Macromolecules* **1993**, *26*, 7058.

(15) Loesche, M.; Schmitt, J.; Decher, G.; Bouwman, W. G.; Kjaer, K. *Macromolecules* **1998**, *31*, 8893.

(16) Steitz, R.; Leiner, V.; Siebrecht, R.; Klitzing, R. *Colloids Surf., A* **2000**, *163*, 63.

(17) Kugler, R.; Schmitt, J.; Knoll, W. *Macromol. Chem. Phys.* **2002**, *203*, 413.

achieved by varying the effective scattering length density (SLD) of a solvent mixture to equal zero. This ability to control the SLD of the solvent is unique to neutron reflectivity, since one can select among chemically identical isotopes that have different neutron scattering lengths. Although controlling the SLD of the environment is commonly employed in studies with biological systems, this technique has not been commonly used in the study of multilayer films. The ability to tune the solvent scattering properties (by controlling the hydrogen-to-deuterium mix) without affecting chemical properties has enabled water distributions to be examined in detail.

Experimental Section

Materials and Film Assembly. PAA (MW = 90 000), and PAH (MW = 60 000) (PAH) were obtained from Polysciences and Aldrich, respectively. Polyelectrolyte solutions of 10^{-2} M (concentration based on monomer unit) were prepared in $18.2 \text{ M}\Omega\cdot\text{cm}$ Millipore water. Multilayer films were fabricated according to the usual layer-by-layer technique using an automated dipper.^{18,19} Polished Si (100) silicon wafers (~ 100 mm in diameter and ~ 6 mm thick) purchased from Wafer World, Inc. were used as substrates and were cleaned in concentrated chromium(III) oxide/sulfuric acid for at least 12 h. The films were first thoroughly rinsed with deionized (DI) water and then rinsed with Millipore water. The pH of the polyelectrolyte solution was adjusted with HCl to a pH of 3.5 for both the polycation and polyanion solutions. An alternating series of polycation and polyanion layers was deposited by immersing the wafers for 15 min into the polyelectrolyte solutions. Between each adsorption step, the wafer was successively immersed into three rinse baths of Millipore water for 1, 2, and 2 min, respectively. The process was repeated until the desired layer thickness of ~ 800 Å was achieved (18 bilayers). After the films were assembled, excess water was removed under a stream of compressed nitrogen. The assembled films were then oven dried under vacuum at 65 °C overnight. The films were then stored under vacuum until placed into the environmental sample chamber for measurement.

Neutron Reflectometry and Data Analysis. The reflectivity experiments were performed at the Chalk River Laboratories (National Research Council, Canada) on the C5 spectrometer at a neutron wavelength of 2.37 Å. Measurements were performed in the specular reflection mode, and the momentum transfer, $q_z = (4\pi/\lambda) \sin \theta$, was varied by scanning in the q_z range of 0.006 Å⁻¹ to 0.08 Å⁻¹. The collimation slits were varied throughout the scan to ensure that the illuminated sample area remained the same and defined the instrument resolution at $\Delta q_z/q_z = 0.045$. The background scattering was measured off-specularly with a fixed angular displacement of the sample of -1° for the humidity cell and -0.15° for the liquid cell. Measurements were performed in three q_z regions: $q_z = 0.08$ – 0.048 Å⁻¹, $q_z = 0.052$ – 0.018 Å⁻¹, and $q_z = 0.022$ – 0.006 Å⁻¹. The overlaps between the three regions are used to match up the intensities in the separate regions. The data were normalized by the incident beam intensity to account for variations due to slit widths. The count time in the high q_z regions (0.08 – 0.018 Å⁻¹) was increased to maintain proper count statistics throughout the entire scan. The samples were placed into an environmental chamber where the humidity, temperature, and solvent conditions could be controlled. The properties of this sample cell and its ability to precisely maintain constant humidity has been fully characterized previously.²⁰ The sample stage was maintained at 25 °C for all experiments. For dry scans, the PAH/PAA films were kept dry in the cell with a nitrogen purge. Controlled humidity environments for films prior to measurement and while in the sample cell were established by using the equilibrium water vapor over saturated salt solutions.²¹ The samples

were allowed to equilibrate for a minimum of 12 h in the humidity chamber prior to any measurements. Bulk water and humidity swelling studies were carried out using 100% D₂O. Dried films were obtained by placing the sample under vacuum for 16 h at 65 °C, and purged with nitrogen while in the sample cell after the films had been H–D exchange equilibrated by exposure to D₂O vapor before drying. To deconvolute the contributions from the swollen PEM matrix and from water uptake within the film, swelling experiments were also conducted using a water/solvent mixture of 92:8 H₂O/D₂O. This solvent mixture has a net SLD of zero, and hence only the PEM matrix contributes to scattering. The water distribution within the film was then obtained by simply subtracting the SLD profile from the original (100% D₂O) scattering curve. Although water and deuterium oxide have slightly different kinetic properties, they possess largely similar thermodynamic properties, and the chemical potentials can be assumed to be equivalent.¹⁷ In the case where bulk water with a solvent mixture of 92:8 H₂O/D₂O was used, the lack of a critical edge required the reflectivity curve to be normalized with the corresponding 100% D₂O normalization factor. The SLD profiles of the films were fitted with Parratt's dynamic approach,²² using the Parratt32 fitting software (provide by HMI). The instrumental resolution was included when fitting the reflectivity curves. The silicon oxide thickness and roughness was fitted from neutron reflectivity curves on bare Si wafers of the same batches as those used as substrates for multilayering. Details of the fit parameters are provided as Supporting Information. Errors on the structural parameters were determined by varying the fit parameter based on a 10% increase in χ^2 , and a Patterson analysis of the reflectivity data was also carried out.²³ Patterson analysis of the reflectivity data, however, was limited by the fact that the experiments were only conducted to $q_z = 0.08$ Å⁻¹, and resolution limitations made it difficult to assess the sharpness at the polymer surface independently from this fit. The correlation distances of the interface using this analysis, however, were similar to the SLD profile interface estimates obtained from the fits using Parratt32, and support well our interpretation by the primary fitting method and analysis presented here. In all cases, the presented solution represents a minimum that was obtained using a variety of initial parameter conditions, fixing each parameter off-minimum in turn, and adjusting all other fit parameters. This variation of each parameter (or combination of parameters) from the minimum, with subsequent iterative fitting, recovered the same global minimum.

Results and Discussion

Figures 1 and 2 show the raw neutron reflectivity data of PAH/PAA samples and best fits to a four-slab model in which the properties of the Si substrate were kept constant. The spectra contain numerous Kiessig oscillations to $q_z = 0.08$ Å⁻¹, suggesting that the films are of uniform thickness, which can be determined by $2\pi/\Delta q_z$, where Δq_z is the distance between two successive fringes. A simple one-box or two-box model of the polymer film was insufficient in producing reasonable fits to the data, especially for the cases where the samples were hydrated. In the case of the humidity-swollen films, a low-SLD outer layer was added to account for chain extension into the ambient environment.

In the case of dry films, additional narrow boxes at the polymer/substrate and the polymer/environment interfaces were required to obtain best fits, and one large slab was used to model the bulk interior of the multilayer. Fits obtained for the bulk water experiments could be fit by subdividing the film bulk into three subregions of slightly changing SLD.

The resulting SLD profile, however, was found to contain step features that were artifacts of the fitting method. A gradient model was then used instead, where the bulk interior of the multilayer was modeled using a sigmoidal function. The resulting

(18) Shiratori, S. S.; Rubner, M. F. *Macromolecules* **2000**, *33*, 4213.

(19) Yoo, D.; Shiratori, S. S.; Rubner, M. F. *Macromolecules* **1998**, *31*, 4309.

(20) Harroun, T. A.; Fritzsche, H.; Watson, M. J.; Yager, K. G.; Tanchak, O. M.; Barrett, C. J.; Katsaras, J. *Rev. Sci. Instrum.* **2005**, *76*, 065101.

(21) Lide, D. R. *CRC Handbook of Chemistry and Physics*, 83rd ed.; CRC Press: Boca Raton, FL, 2002.

(22) Parratt, L. G. *Phys. Rev.* **1954**, *95*, 359.

(23) Crowley, T. L.; Lee, E. M.; Simister, E. A.; Thomas, R. K. *Physica B* **1991**, *173*, 143.

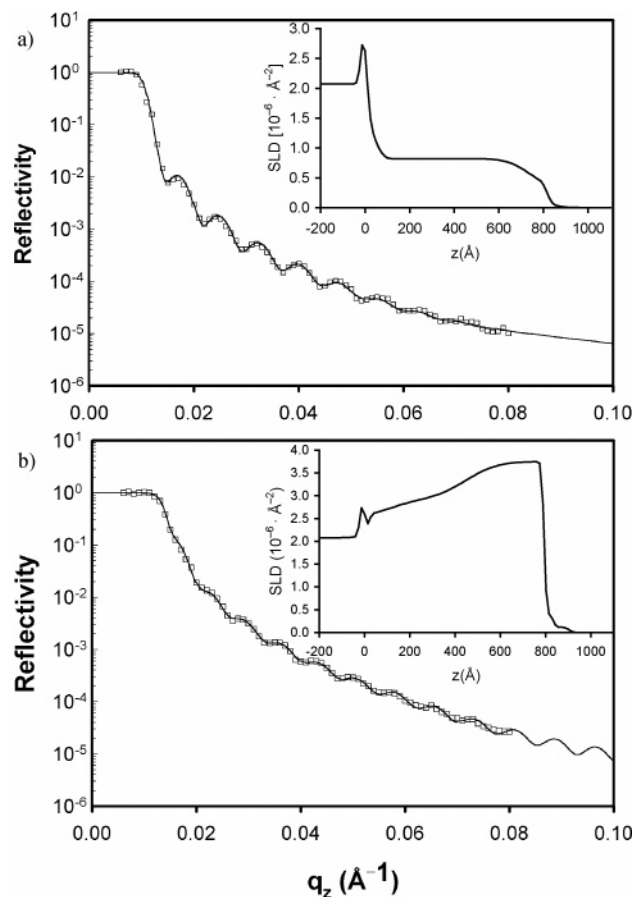


Figure 1. Neutron reflectivity data (error bars are within the size of the symbols) and fit (solid continuous line) for an assembly pH = 3.5 PAA/PAH multilayer film (a) in the dry state and (b) exposed to 11% RH with a 100% D₂O content. The corresponding SLD profile of the model is shown in the inset.

fit was as good as that of the four-box model, and produced a similar SLD profile. All parameters (film/substrate roughness, internal roughness, film/air roughness, and the SLD of the polymer slabs) were free to evolve, except for the SLD of the substrate and oxide, and produced physically reasonable fits. In the resulting SLD profiles of the multilayer films, we chose to define $z = 0$ as the silicon/oxide film interface, and the multilayer film can be described well using a three-region model of nominal thickness $794 \pm 15 \text{ \AA}$ (determined from the midpoint of the diffuse polymer-air interface). The SLD profile indicates that the free surface was quite diffuse, and that the bulk of the film is best described by a smooth and flat profile. The absence of oscillations in the profile shows that the bulk multilayer structure is evidently highly interpenetrated, consistent with previous investigations.^{14,15} The spike seen at $z = 0$ is attributed to the high SLD ($3.475 \times 10^{-6} \text{ \AA}^{-2}$) of the SiO₂ layer. However, the film-substrate interface appears to have an SLD measurably higher than that of the film bulk. This increased SLD near the substrate interface is likely due to a higher density of polymer material, which is consistent with other literature suggestions. Conceivably, the increased SLD could also be due to a localization of counterions, but accounting for the increased SLD near the substrate ($1.5 \times 10^{-6} \text{ \AA}^{-2}$, as compared to $0.7 \times 10^{-6} \text{ \AA}^{-2}$ in the film bulk) would require, for example, $\sim 6 \text{ Na}^+$ ions per PAA group. The films studied were assembled at pH = 3.5, and, under these conditions, PAH is fully charged and PAA is partiality ionized ($\sim 76\%$).^{14,20} Given that only $\sim 25\%$ of the PAA groups are available for bonding to counterions (the rest form ionic cross-links), it does not seem

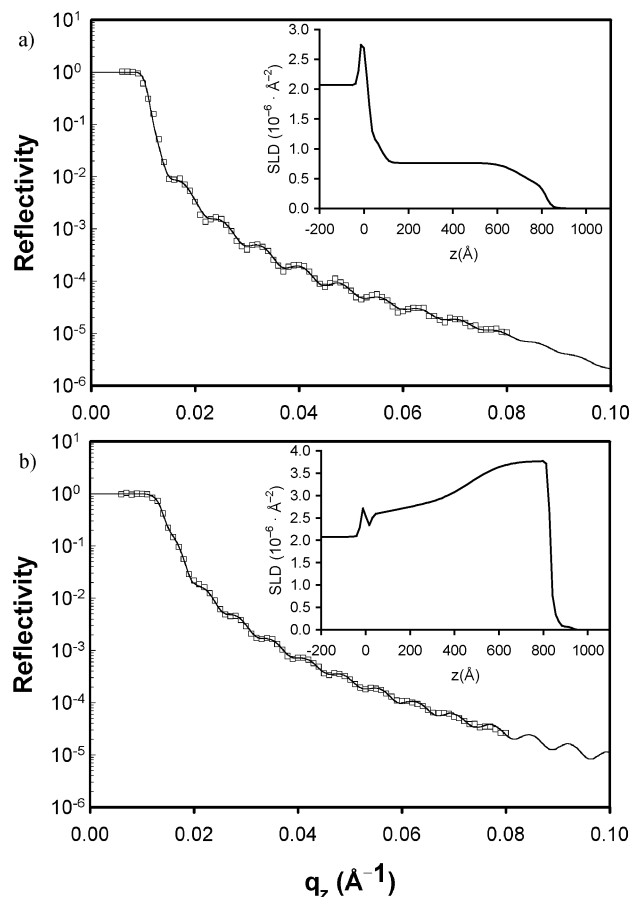


Figure 2. Neutron reflectivity data (error bars are within the size of the symbols) and fit (solid continuous line) for an assembly pH = 3.5 PAA/PAH multilayer film (a) exposed to 11% RH with a solvent vapor mix of 92:8 (H₂O/D₂O) and (b) exposed to 43% RH with a 100% D₂O content. The corresponding SLD profile of the model is shown in the inset.

reasonable to suggest that the increased SLD is due to counterions alone.

The films assembled at pH = 3.5 can be viewed as a mesh of many voids in which water molecules absorb. The incorporation of deuterium oxide vapor into the film, which has a large positive scattering ($\text{SLD} = 6.4 \times 10^{-6} \text{ \AA}^{-2}$), leads to an increase in the SLD of the multilayer as seen in Figures 1b and 2b. A single-slab model could not describe films swollen in a humid atmosphere, and an internal asymmetry in the film was necessary to reproduce the experimental reflectivity profiles. However, it is difficult to determine whether the contribution to the SLD profile is due to film swelling or sorption of D₂O vapor. To determine the SLD profile of the PEM at 11% RH, a vapor solvent mixture of 92:8 H₂O/D₂O was used. When the multilayer was exposed to this environment, only the film contributed to scattering since this solvent mixture has an effective SLD of zero. The resulting SLD profile is shown in Figure 2a, and is very similar to that of polymer in the dry state (Figure 1a), indicating that the multilayer does not swell to an appreciable extent. As inferred from the dry and 11% RH (92:8 H₂O/D₂O) SLD profiles, the extent of H/D exchange in the film was negligible, even when exposed to 100% D₂O vapor. It is plausible that, at this low humidity, the osmotic stress is insufficient to induce film swelling. The low water fraction in the film (and hence the low extent of swelling) limits the amount of exchangeable water available to the film. The SLD profile of water within the film was then deconvoluted from the contributions due to the film and water in the original 11% RH (100% D₂O) scattering curve, and is shown in Figure 3. It is clear

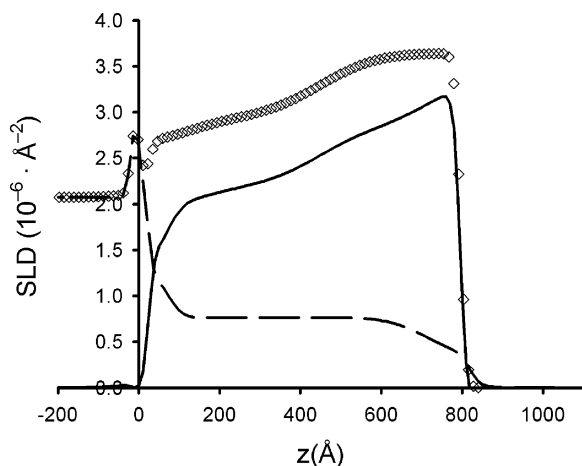


Figure 3. SLD profile of the neutron reflectivity data for a multilayer film exposed at 11% RH. The open symbols correspond to the model at 11% RH (100% D₂O), the dashed line corresponds to the SLD profile at 11% RH (92:8 solvent mix of H₂O/D₂O), and the black solid line is the difference of the SLD profiles and indicates the water distribution within the film.

that the water distribution within the multilayer is asymmetrical; the water vapor is strongly localized at the film–air interface and does not penetrate to the substrate. Ellipsometry studies on films of similar thickness exposed to 11% RH have shown an $\sim 1.15\%$ increase in thickness. Defining the absolute thickness of the sample is nontrivial because of the fuzzy interface resulting from the polyelectrolyte's loops and tails that extend into the humid environment. For this reason, we chose to determine the film thickness at the midpoint of the bulk polymer–air interface. For the profile of the 11% RH (100% D₂O) film, the thickness was observed to have increased by $0.45 \pm 0.03\%$. In contrast, the thickness determined with ellipsometry was modeled as a single slab and did not take into account the internal density gradient of water vapor, nor did it accurately interpret the diffuse surface. These factors may lead to an inaccurate determination of the optical properties of the film by this technique, but the extent of swelling using the two techniques is still quite similar. Neutron experiments also show that exposures to 43% RH (100% D₂O) leads to a $4.98 \pm 0.03\%$ increase in thickness (834 ± 16 Å), as indicated in Figure 2b. There was sufficient osmotic stress induced on the polymer network to expand to a greater extent than when exposed to 11% RH. The polymer/air interface is sharp, as seen in the SLD profile, and is an indication that water is localized preferentially at the surface. Ellipsometry studies on films exposed to 43% RH have shown a $\sim 4.2\%$ increase in thickness, which is consistent with the neutron reflectivity results presented here.

The asymmetrical water distribution in the PEM and the relatively sharp boundary at the polymer–air interface may contain clues of the strong effect of water vapor adsorption on the swelling kinetics with bulk water. For instance, bulk water swelling studies on multilayers assembled at pH = 3.5 required ~ 3 s to reach equilibrium when the film was preexposed to an environment of 20% RH, whereas, when the film was equilibrated at 45% RH, ~ 1800 s were required to reach maximum swelling.¹² Water molecules are likely in constant motion, but the hydrophobic interactions of the PAH and PAA polymer backbone may well force the water molecules into a more rigid organized cluster of hydrogen-bonded molecules, whereas the free carboxylic acid groups of the PAA would participate in a hydrogen-bonding network.²⁴ This effect serves to increase the structural organization of water and thus decreases the entropy of the water

molecules in the clusters. The relatively sharp interface (Figure 3) strongly suggests that water is segregated at the film–vapor interface. As shown in the Supporting Information (Figure 1S), the fit is sensitive to the bulk interfacial roughness. An increase in the surface roughness of only 5 Å is sufficient to cause a substantial deviation from the fit, indicating the requirement for the sharp interface. Water localization at the film–air interface might also be ascribed to surface tension effects; however, this is not likely the case, as will be shown later.

The asymmetrical water distribution cannot be explained with a simple diffusion model where water penetrates in a passive manner through the pores of the PEM. Our results support the notion that the outer layers are more diffuse than the interior of the multilayer,^{10,25} as indicated by the SLD profile of the dry film (Figure 1a), and indeed more water vapor is associated with the outer layer (Figure 3), which is consistent with previous investigations.^{13,16,26} However, a simple percolation model would predict a constant water distribution through the bulk region of the film that extends to the substrate, which is not the case, as our results clearly indicate that the water vapor does not penetrate to the substrate and is distributed asymmetrically throughout the film. Furthermore, this model would fail to explain the water localization at the polymer–air interface. The water gradient that forms in the film can be explained through kinetic arguments though. Essentially, water adsorbs at the free surface of the film and blocks accessible microchannels in the film, thereby inhibiting further diffusion of the vapor. If this were strictly a surface phenomenon, the water distribution within the film would eventually saturate and have a uniform profile throughout the film. However, ellipsometry studies on PEMs of similar thickness exposed to 11% RH indicate that the exposure times used in these experiments is sufficient for the film to reach saturation. Furthermore, a partial scan ($q_z = 0.022 - 0.006$ Å⁻¹) was taken ~ 11 h prior to the full scan. The partial and full scans overlap each other, indicating that the film was equilibrated. Insufficient exposure time would have resulted in an observable shift in the critical edge to higher q_z . If the drying process, after exposure to D₂O vapor, was not uniform or incomplete, an observable asymmetry in the film SLD would have also been observed in the 11% RH (92:8 solvent mix of H₂O/D₂O) experiment (because of the higher scattering contrast of deuterium). We must stress that the resultant profiles represent the multilayers at equilibrium and are not merely a snapshot of the diffusion process or isotopic exchange. It is therefore more likely that water clusters would form a gradient throughout the film, which would further restrict the motion of water vapor and establish a chemical gradient through the film. As the vapor front moves through the film, the formation of water clusters would impede the diffusion of more water into the microchannels of the subphase, resulting in less water being available to the underlying layers. This is clearly shown in the SLD water profile within the film, where vapor does not penetrate to the substrate–polymer interface. Swelling studies with bulk water suggest that the interior of the PEM is less restrictive than the outer surface layers. Upon exposure to bulk water, the film gradually expands, but only to a modest extent. After a relatively long induction period, which is dependent on the preexposure humidity, the rate of swelling abruptly increases until eventually a constant rate of swelling is established. PEM swelling dynamics supports the idea of a gradient of water

(24) Israelachvili, J. N. *Intermolecular and Surface Forces: With Applications to Colloidal and Biological Systems*; Academic Press: London; San Diego, CA, 1985.

(25) Wong, J. E.; Rehfeldt, F.; Haenni, P.; Tanaka, M.; Klitzing, R. v. *Macromolecules* **2004**, *37*, 7285.

(26) Plech, A.; Salditt, T.; Munster, C.; Peisl, J. J. *Colloid Interface Sci.* **2000**, *223*, 74.

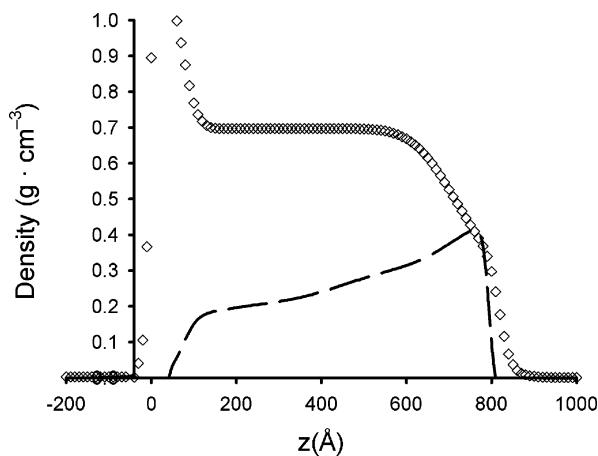


Figure 4. Film density and water distribution for a multilayer film exposed at 11% RH. The open symbols correspond to the film density, and the dashed line corresponds to the water fraction distribution within the film.

clusters through the film, where water is found to preferentially localize at the PEM surface. This asymmetric water distribution may also be due to the formation of a pK_a gradient in the film during assembly, characterized previously.²⁰ As layers are added, the apparent pK_a of the PAA shifts to lower values, where the surface layers are more ionized than those within the film. The free carboxylic acid groups at the surface of the film would therefore associate with the water clusters through hydrogen bonding, which results in a higher concentration of water near the surface. The degree of ionization decreases upon approach to the substrate, as fewer carboxylic acid groups are available to aid in the formation of water clusters, and a gradient in the water distribution results. In either case, these effects are more pronounced at higher humidity and lead to a longer time scale for the diffusion, but the osmotic stress is larger, and the polymer network expands. It is therefore conceivable that the diffusion of bulk water would be hindered through the blockage of accessible microchannels in the film, through the formation of hydrogen-bonded water clusters, and this effect would lead to longer time scales being required to reach saturation with increasing humidity. More importantly, the gradient of water clustering would explain the long induction time required to establish a late-stage acceleration in swelling due to autocatalytic plasticization of the film, as observed in kinetic studies.

The SLD values produced from the fits of the reflectivity curves for PEM films are consistent with those reported previously in the literature.^{15,17,27} The physical density and corresponding water fraction distribution in the PEM are shown in Figure 4, where the density profiles were calculated using an association stoichiometry of PAA to PAH, with the PAA ionized to ~76%. This percent ionization is based upon literature reports of the effective pK_a of PAA chains in PAA/PAH multilayers (where an apparent $pK_a = 3$ was observed)²⁸ and is consistent with Fourier transform infrared (FTIR) measurements of PAA ionization in multilayers.¹⁸ The association of counterions was omitted in the calculations since it was presumed that they would have been exchanged with H (or D) ions during assembly. The extent of exchange in the films appeared to be negligible and was then assumed to be zero for the fitting. On this basis, the average physical density of the bulk interior of the PEM was determined to be $0.8 \pm 0.1 \text{ g} \cdot \text{cm}^{-3}$, which is reasonable

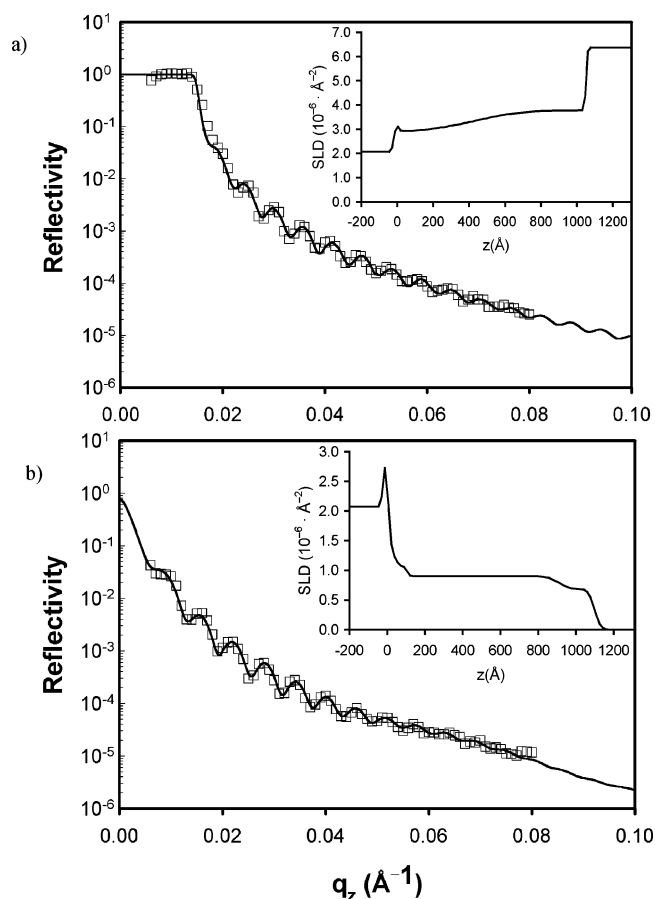


Figure 5. Neutron reflectivity data (error bars are within the size of the symbols) and fit (solid continuous line) for a multilayer film (a) exposed to 100% bulk D_2O and (b) exposed to bulk water with a solvent mix of 92:8 (H_2O/D_2O). The corresponding SLD profile of the model is shown in the inset.

considering that, under the assembly conditions, the PEM forms a loose structure and is consistent with measurements on PAH/PSS multilayers, where densities of $\sim 0.8\text{--}1.1 \text{ g} \cdot \text{cm}^{-3}$ were deduced.^{15,26,29,30} As indicated, the polymer–air interface is diffuse, whereas, at the substrate interface, the multilayer is more dense than it is in the bulk. This densification is presumably due to substrate effects during the assembly of the few first layers. The water density associated to the diffuse outer layer is ~40% of that of bulk water, whereas the water content ranged from 30 to 20% in the bulk of the film.

The distribution of bulk water was also studied. Neutron reflectivity data, fits, and the corresponding SLD profiles of the PEM exposed to pure D_2O and to the solvent mixture of 92:8 H_2O/D_2O are shown in Figure 5. When exposed to bulk water, the SLD profiles reveal that the multilayer film swells considerably to $1071 \pm 13 \text{ \AA}$, with an extent of swelling of $34.87 \pm 0.03\%$, which is consistent with other reports in the literature, which range from ~20% to 40%.^{15,27}

The profile of water within the film was again deconvoluted from the contributions due to the film (92:8 $H_2O:D_2O$) and water in the original 100% D_2O scattering curve, as shown in Figure 6. The resultant water distribution in films swollen with bulk solvent is again asymmetric. Here again, a relatively sharp film–ambient interface is observed, and water is preferentially found

(27) Glinel, K.; Prevot, M.; Krustev, R.; Sukhorukov, G. B.; Jonas, A. M.; Moehwald, H. *Langmuir* **2004**, *20*, 4898.

(28) Burke, S. E.; Barrett, C. J. *Langmuir* **2003**, *19*, 3297.

(29) Tarabia, M.; Hong, H.; Davidov, D.; Kirstein, S.; Steitz, R.; Neumann, R.; Avny, Y. *J. Appl. Phys.* **1998**, *83*, 725.

(30) Steitz, R.; Leiner, V.; Tauer, K.; Khrenov, V.; Klitzing, R. V. *Appl. Phys. A: Mater. Sci. Process.* **2002**, *74*, S519.

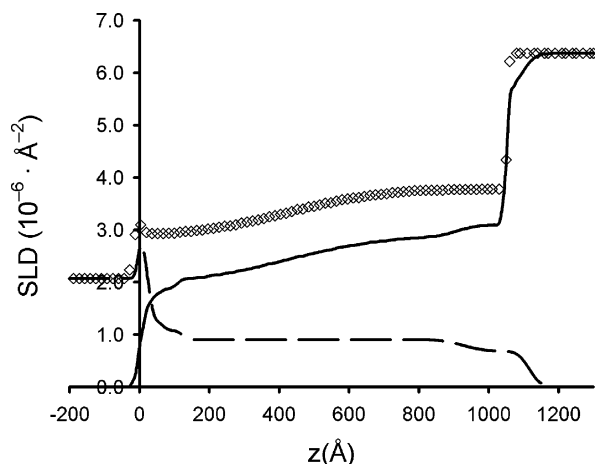


Figure 6. SLD profile of the neutron reflectivity data for a multilayer film exposed to bulk water. The open symbols correspond to the model with 100% D₂O, the dashed line corresponds to the SLD profile with the solvent mix of 92:8 H₂O/D₂O, and the black solid line is the difference of the SLD profiles, which indicates the water distribution within the film.

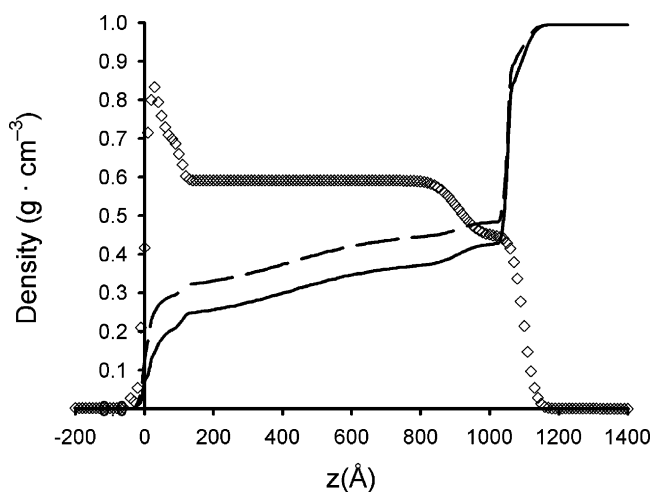


Figure 7. Film density and water distribution for a multilayer film exposed to bulk water. The open symbols correspond to the film density, the dashed line corresponds to the water fraction distribution within the film with the extent of deuteration calculated to 41%, and the solid line corresponds to the water fraction distribution within the film with the extent of deuteration calculated to 100%.

to localize at the film surface, only partially penetrating to the substrate. This implies that surface tension effects are not responsible for the water localization at the surface; the relatively sharp interface is present, even though the film was exposed to bulk water, which is consistent with the formation of water clusters.

The physical density and water fraction distribution in the PEM when exposed to bulk water is shown in Figure 7. The density profile of the PEM was calculated in a manner similar to that used the 11% RH case with an assumed association stoichiometry of PAA (~76% ionized) to PAH. However, when complete D/H exchange was assumed, the overall density of the PEM was higher than that found when it was exposed to water vapor.

Since the mass density of the film is conserved, the resultant bulk interior density of the film should be $0.59 \pm 0.02 \text{ g} \cdot \text{cm}^{-3}$ when swollen to an extent of ~35%. It is known that the kinetics of H₂O to D₂O exchange is faster than that of D₂O to H₂O exchange because of the lower zero-point energy of the D–O

bond. It is therefore conceivable that inefficient isotopic substitution (D to H) occurred in the PEM film because of insufficient solvent exposure time. However, the film SLD for the bulk 92:8 H₂O/D₂O shows no asymmetry and suggests that the exchange event has occurred uniformly in the film. The reflectivity data for the bulk 92:8 H₂O/D₂O experiment was analyzed using data from regions 2 and 3 ($q_z = 0.052\text{--}0.018 \text{ \AA}^{-1}$ and $q_z = 0.022\text{--}0.006 \text{ \AA}^{-1}$) (~5.5 h after the scan in region 1, $q_z = 0.08\text{--}0.048 \text{ \AA}^{-1}$). Fits obtained using the truncated data sets (region 2, and regions 2 and 3) gave profiles similar to that obtained using all three scan regions. The bulk SLD of the film was virtually unchanged and suggests that the exchange process was complete. Analysis of the spacing of the Kiessig fringes from the three regions also indicates that the time scale used in the experiment was sufficient for the exchange process. If the SLD of the film were changing in time, the position of the Kiessig fringes would be changing during scanning, leading to an apparent modification of the fringe shape. The fact that the Kiessig spacing does not change over the measured q_z range indicates that the SLD of the film was constant during the measurement. We can therefore state with confidence that the resultant SLD profile is not due to a kinetic D to H exchange process (kinetic isotope effect), and represents the film at equilibrium. To account for the problem of inefficient D/H exchange, the H/D ratio was calculated on the basis of the assumed physical density and the inferred SLD profile of the film. The extent of the H/D exchange was thus determined to be ~59%. Here again, the polymer–water interface is diffuse, whereas the multilayer is more dense at the polymer/substrate interface than it is in the bulk. It is difficult to know with any certainty the extent of H/D exchange with respect to the 100% D₂O bulk water experiment. The extent of deuteration in the film could range from 100 to 41% (the corresponding water fraction distributions are shown in Figure 7). In either case, the overall water distribution in the film is asymmetrical, similar to the case of exposure to 11% RH. The difference between the two is a decrease of ~8% in the water fraction within the film in the case where exchange is 100%. The water fraction associated with the diffuse outer layer is ~54%, and the water content in the bulk of the film ranges from 45 to 35%. The water content near the polymer/substrate interface is much lower (~18%) than that in the bulk interior of the film. The overall water fraction in the film is higher because of the increase in osmotic stress on the polymer network.

Although there is sufficient osmotic stress to induce expansion of the PEM network, water clusters may still be forming within the film. Arguments similar to those presented in the case of sorption from the gas phase could be applied to the case of swelling with bulk water; however, the effect is not as pronounced as it is in the case of vapor sorption. In this instance, water would permeate quickly through the film since the PEM was swollen from the dry state. As the solvent front moves through the film, the water molecules would associate with the free carboxylic acid groups as well as induce hydrophobic interactions between the polyelectrolyte chains, leading to the formation of a gradient of water clusters that is preferentially localized at the surface. In principle, this would inhibit water from penetrating to the substrate, since the accessible microchannels deep within the film would be blocked.

Conclusions

Neutron reflectivity experiments have provided some the fine details of film swelling and water localization in thin PAH/PAA multilayer films assembled at a pH of 3.5. In particular, the

ability to tune solvent scattering properties (by controlling the hydrogen to deuterium mix) without affecting the chemical properties has enabled water distributions to be examined in detail. It is now apparent that water localizes asymmetrically within multilayer systems both in the gas phase and when swollen with bulk water. In either case, water segregates predominantly at the diffuse free surface. The localization of water at the polymer–air interface can be used to explain anomalous swelling kinetics, where time scales to reach maximum swelling varied from a few seconds to tens of minutes, depending on the preexposed humidity conditions of these novel materials.

Acknowledgment. The authors would like to thank the Canadian Neutron Beam Centre for beam time. Funding was provided by NSERC Canada and the McGill FQRNT Centre for Self-Assembled Chemical Structures.

Supporting Information Available: Figure showing the neutron reflectivity data and fit for an assembly pH = 3.5 PAA/PAH multilayer film exposed to 11% RH with a 100% D₂O content, and tables of the structure parameters of various PAH/PAA films. This material is available free of charge via the Internet at <http://pubs.acs.org>.

LA0529613